



Published in final edited form as:

Arterioscler Thromb Vasc Biol. 2020 January ; 40(1): 72–85. doi:10.1161/ATVBAHA.119.313078.

Replacing saturated fat with unsaturated fat in western diet reduces foamy monocytes and atherosclerosis in male *Ldlr*^{-/-} mice

Zeqin Lian, Xiao-yuan Dai Perrard, Xueying Peng, Joe L. Raya, Alfredo A. Hernandez, Collin G. Johnson, William R. Lagor, Henry J. Pownall, Ron C. Hoogeveen, Scott I. Simon, Frank M. Sacks, Christie M. Ballantyne, Huaizhu Wu

Department of Medicine (Z.L., X.D.P., X.P., J.L.R., C.G.J., R.C.H., C.M.B., H.W.), Department of Molecular Physiology and Biophysics (W.R.L.), Department of Pediatrics (C.M.B., H.W.), and Center for Cardiometabolic Disease Prevention (C.M.B.), Baylor College of Medicine, Houston, TX; Houston Methodist Research Institute, Houston, TX (H.J.P.); Department of Biomedical Engineering, University of California, Davis (A.A.H., S.I.S.); Department of Nutrition, Harvard School of Public Health, and Department of Medicine, Harvard Medical School and Brigham and Women's Hospital, Boston, MA (F.M.S.); and Institute of Materia Medica, Peking Union Medical College Hospital, Chinese Academy of Medical Sciences and Peking Union Medical College, Beijing, China (X.P).

Abstract

Objective: A Mediterranean diet supplemented with olive oil and nuts prevents cardiovascular disease in clinical studies, but the underlying mechanisms are incompletely understood. We investigated whether the preventive effect of the diet could be due to inhibition of atherosclerosis and foamy monocyte formation in *Ldlr*^{-/-} mice fed with a diet in which milkfat in a western diet was replaced with extra-virgin olive oil and nuts (EVOND).

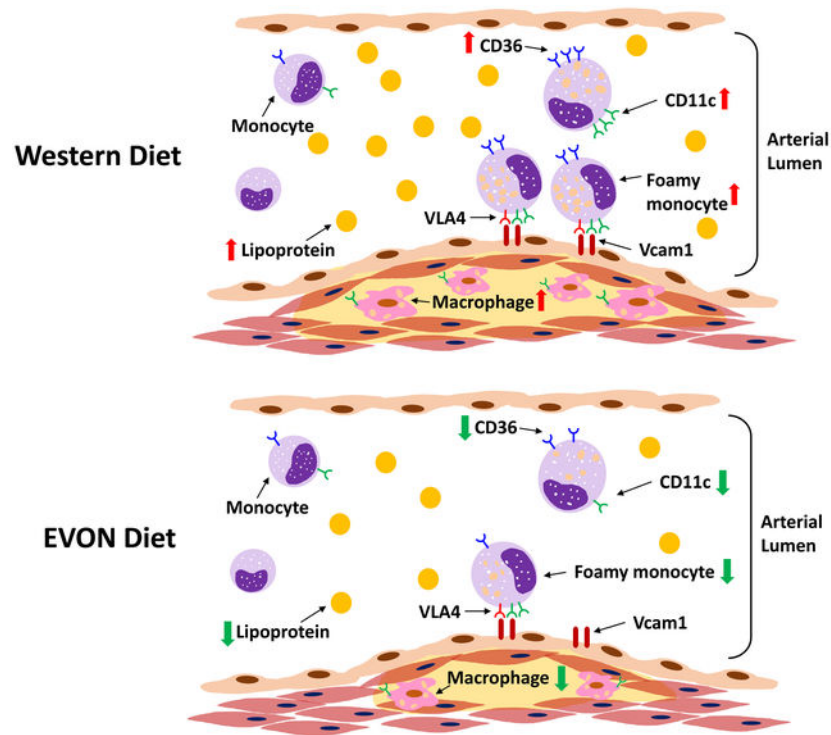
Approach and results: *Ldlr*^{-/-} mice were fed EVOND or a western diet for 3 (or 6) months. Compared to the western diet, EVOND decreased triglyceride and cholesterol levels but increased unsaturated fatty acid concentrations in plasma. EVOND also lowered intracellular lipid accumulation in circulating monocytes, indicating less formation of foamy monocytes, compared with the western diet. In addition, compared to the western diet, EVOND reduced monocyte expression of inflammatory cytokines, CD36, and CD11c, with decreased monocyte uptake of oxidized LDL *ex vivo* and reduced CD11c⁺ foamy monocyte firm arrest on vascular cell adhesion molecule-1- and E-selectin-coated slides in an *ex vivo* shear flow assay. Along with these changes, EVOND compared to the western diet reduced the number of CD11c⁺ macrophages in atherosclerotic lesions and lowered atherosclerotic lesion area of the whole aorta and aortic sinus.

Correspondence to Huaizhu Wu, MD, Baylor College of Medicine, One Baylor Plaza, Room 526D, MS: BCM285, Houston, TX 77030. hwu@bcm.edu.

Disclosures
None.

Conclusion: A diet enriched in extra-virgin olive oil and nuts, compared to a western diet high in saturated fat, lowered plasma cholesterol and triglyceride levels, inhibited foamy monocyte formation, inflammation, and adhesion, and reduced atherosclerosis in *Ldlr*^{-/-} mice.

Graphical Abstract



Keywords

High-unsaturated fat diet; Foamy monocyte; Atherosclerosis

Introduction

The Prevención con Dieta Mediterránea (PREDIMED) clinical trial demonstrated that a Mediterranean diet supplemented with extra-virgin olive oil or nuts, which are rich in unsaturated fatty acids (UFAs), including monounsaturated fatty acids (MUFAs) and polyunsaturated fatty acids (PUFAs), reduced the incidence of major cardiovascular events in a high cardiovascular risk population.¹ Accumulating evidence supports the benefit of dietary UFAs over saturated fatty acids (SFAs) to improve cardiovascular health.^{2, 3} However, the mechanisms by which UFAs reduce the risk for atherosclerotic cardiovascular disease have not been fully defined.

Atherosclerosis is an inflammatory process. Recently, the Canakinumab Anti-inflammatory Thrombosis Outcomes Study (CANTOS) showed benefits of an inflammation-targeting therapy on reducing the risk for recurrent atherosclerotic cardiovascular events.⁴ Monocytes, a critical component of the innate immune system, quickly respond to changes in plasma lipids and contribute to atherogenesis by infiltrating the sub-endothelial space of arterial

walls, where they form inflammatory macrophage foam cells.^{5–12} Our previous studies showed that a western diet (WD; 21% milkfat, high SFAs and cholesterol) induces formation of circulating foamy monocytes (FM), which contain intracellular lipid droplets, express high levels of CD11c and CD36, present with inflammatory phenotypes, and contribute to atherogenesis in animal models.^{7, 8} FM also exist in the circulation of humans with hyperlipidemia, including familial hypercholesterolemia or postprandial hypertriglyceridemia, and may contribute to atherosclerosis.^{12, 13} However, how high-UFA diet affects FM formation and phenotypes is still poorly understood.

In the present study, we fed *Ldlr*^{-/-} mice either a WD or a diet in which milkfat in WD was replaced with extra-virgin olive oil and nuts (EVON), the so-called EVON diet (EVOND), and then examined FM formation, monocyte phenotypes, and extent of atherosclerosis.

The EVOND-fed mice showed lower plasma total triglyceride (TG) and cholesterol levels, but higher plasma UFA levels, than WD-fed mice. Compared to those from WD-fed mice, monocytes from EVOND-fed mice had less lipid accumulation, decreased adhesion to endothelial cell adhesion molecules, and reduced uptake of oxidized low-density lipoprotein (oxLDL). Compared to WD, EVOND decreased atherosclerosis development in these mice.

Materials and Methods

The data that support the findings of this study are available from the corresponding author upon reasonable request.

Animals and diets

To avoid the potential confounding effects of estrogen on lipid metabolism and atherosclerosis development,^{14–16} male *Ldlr*^{-/-} mice (The Jackson Laboratory, stock number: 002207-B6.129S7-*Ldlr*^{tm1Her/J}) were used and maintained in an environmentally controlled animal facility at Baylor College of Medicine. All animal studies were approved by the Institutional Animal Care and Use Committee of Baylor College of Medicine. Mice were either fed a normal laboratory diet (ND) throughout or switched to WD (21% milkfat, 0.2% cholesterol; Dyet 112734, Dyets Inc) or EVOND (21% total fat from extra-virgin olive oil, walnuts, almonds, and hazelnuts; 0.2% cholesterol) at age 8 weeks and maintained on WD or EVOND for 3 months unless stated otherwise. EVOND was a customized diet from Dyets Inc (Supplemental Table I); the major fatty acid (FA) profile was analyzed by gas chromatography–mass spectrometry (GC-MS, see below), which showed that percentages of MUFAs and PUFAs in total measured FAs were higher and the SFA percentage was lower in EVOND than in WD (Supplemental Table II). Plasma lipid levels were determined from blood drawn via facial vein puncture after 6-h fast, and plasma glucose, total cholesterol and TG levels were measured enzymatically (Wako Diagnostics). Fasting plasma insulin levels were determined by ELISA kit (Millipore Sigma). Plasma malondialdehyde (MDA) level was determined by TBARS assay kit (Cayman Chemical). Mouse body composition was assayed by small animal MRI (Lunar Corporation). For insulin tolerance test (ITT), mice were fasted for 6 h and then were injected i.p. with 1.25 U/kg regular human insulin (Novo Nordisk). Blood glucose levels were measured before and at 30 to 120 min after injection by glucometer (Bayer Contour).¹⁷

Plasma FA and lipoprotein profiles

For FA profiling by GC-MS, plasma samples from mice were hydrolyzed with 0.5% NaOH for 2 h and then delipidated by organic solvent extraction (CHCl₃-CH₃OH, 2:1, v/v) to yield total hydrolyzed FAs. In addition, split plasma samples were also analyzed by GC-MS for nonesterified FAs (NEFAs). Both total FAs and NEFAs were derivatized with methanol-acetyl chloride (50:1 (v/v)) to yield methylated FAs. FA methyl esters were analyzed by gas chromatography on a fused silica capillary column (Alltech, Deerfield, IL.; 30 m × 0.25 mm × 0.25 μm film). Analysis was performed on a Hewlett-Packard 6890GC coupled to a 5973 Mass Selective Detector as previously described.^{18, 19} Dietary FA composition was also examined by the above procedure.

Plasma lipoprotein profiles were determined by size exclusion chromatography (SEC, Superose HR6 column; GE Health) of 200 μL plasma per mouse as previously described.²⁰ Cholesterol and TG concentrations of each fraction were determined enzymatically (Wako Diagnostics).

Quantitative polymerase chain reaction (qPCR) analysis

To analyze gene expression, total RNA was isolated from tissues using TRIzol™ reagent (Life Technologies) and an RNA miniprep Kit (Zymo Research) and subjected to qPCR on StepOne plus system with SYBR Green dye (Applied Biosystem). mRNA levels of target genes were normalized to GAPDH. Primer sequences were cited from Primerbank and are shown in Supplemental Table III.²¹

Antibodies and fluorescence-activated cell sorter (FACS) analysis of circulating monocytes

For FACS analysis, monoclonal antibodies against the following mouse antigens were used: CD115 (PE, AFS98, eBioscience), CD204 (FITC, 2F8, Bio-Rad Laboratories), CD11c (PerCP-Cy5.5, N418, eBioscience), CD36 (FITC, MF3, Bio-Rad Laboratories), Ly-6C (APC, HK1.4, eBioscience), TNFα (PE, MP6-XT22, eBioscience), and IL-1β (PE, NJTEN3, eBioscience). For cell surface staining,^{7, 8} blood samples were diluted with equal volume of phosphate-buffered saline (PBS) supplemented with 0.5% bovine serum albumin (BSA) and incubated with fluorescence-conjugated monoclonal antibodies or with appropriate isotype negative controls for 30 min. After washing with PBS, the samples were incubated with BD FACS Lysing Solution (BD Biosciences) for 10 min then washed with PBS again. For Nile red staining, after red blood cells were lysed, cells were stained with Nile red (0.1 μM) for 20 min and then washed twice with PBS. For intracellular staining,^{13, 22} 100 μL blood was incubated with 5 μg/mL lipopolysaccharide (LPS) plus Golgi plug (BD bioscience) for 4 h, then stained for TNFα or IL-1β following the intracellular staining protocol of BD cytofix/cytoperm plus kit. After staining, all samples were resuspended in 2% paraformaldehyde in PBS. Data were collected by a BD LSR II cytometer and analyzed using Kaluza software (Beckman Coulter). Monocytes and subsets were identified following the same strategy as described previously.^{7, 8} Briefly, CD115⁺ or CD204⁺ leukocytes were defined as total monocytes. Monocyte subsets were identified using the combination staining of CD115, CD11c, CD36, and Ly-6C, with corresponding isotypes as negative controls (Supplemental Figure I).

Triglyceride-rich lipoprotein (TGRL) treatment and oxLDL uptake assay

TGRL fraction (density <1.006 g/mL) was floated and isolated from plasma of mice fed WD or EVOND by ultracentrifugation. TG and cholesterol concentrations in TGRLs were determined enzymatically. EDTA-anticoagulated blood (100 μ L) from *Ldlr*^{-/-} mice on ND was washed and resuspended in RPMI-1640 medium, then incubated for 4 h with TGRL fraction at 200 mg/dL of TG. To determine the effects of FAs derived from TGRLs on monocyte phenotypic changes, TGRL fractions (equal to 200 mg/dL of TG) were treated with 2 U/mL lipoprotein lipase (LPL) for 30 minutes at 37°C, then lipolysis products were immediately added to medium and incubated with washed blood (from *Ldlr*^{-/-} mice on ND) for an additional 4 h.²³ After incubation, monocytes were surface stained for FACS analyses.

For ex vivo monocyte oxLDL uptake assay, mouse whole blood was used and endogenous lipoproteins were removed from blood by centrifugation and washing with PBS. Then, cell pellets were resuspended in RPMI1640 medium and were incubated at 37°C with DiI-labeled oxLDL (Kalen Biomedical) at 0.05 mg/mL for 1 h, with or without 4 μ g/mL of an anti-mCD36 antibody (Abcam). Monocyte DiI-oxLDL uptake was detected by FACS after staining with FITC-anti-CD204 antibodies.

Ex vivo micro-flow adhesion assay

Design and assembly of the microfluidic device and the whole blood adhesion assay were performed as previously reported.²⁴ Briefly, clean coverslips that were coated with recombinant mouse VCAM-1/Fc chimera and E-selectin/Fc chimera (R&D Systems) were assembled with a 4-channel PDMS device and kept on a 37°C surface. Peripheral blood (0.1 mL) was drawn into heparin-coated tubes via facial vein puncture and incubated with PE-anti-CD115 and FITC-anti-CD11c antibodies (with corresponding isotypes as negative controls, Supplemental Figure II) at room temperature for 20 min. Then, after 1:3 dilution in PBS with calcium and magnesium, 60 μ L diluted blood was introduced into the channel at a flow rate that produced a shear stress of 2 dynes/cm² at fluid-glass interface. Blood was perfused through the chamber for 5 min followed by fixation and mounting in medium containing DAPI. The number of adherent “foamy” (CD115⁺CD11c⁺) monocytes was counted and normalized by total infused monocyte number.

Analysis of atherosclerotic lesions

For the mouse atherosclerosis study, we adhered to the guidelines for experimental atherosclerosis studies as described in the American Heart Association Statement.^{7, 8, 25–27} Briefly, the aortae were dissected and fixed in 4% paraformaldehyde/PBS, and then cut and pinned longitudinally on a black pad and stained with oil red O; digital images were captured with a Nikon camera. Atherosclerotic lesion areas that were oil red O positive were quantitated using ImageJ analysis software and expressed as percentage relative to the whole aortae.

For aortic sinus monocyte/macrophage analysis, mouse hearts were harvested and embedded in Tissue Tek optimal cutting temperature (OCT) medium (Sakura Finetek). Tissue sections (5 μ m thickness) were acquired from the initial appearance of the aortic valves. Serial sections were collected on consecutive slides. For fluorescent immunostaining, the sections

were fixed in 4% paraformaldehyde in PBS for 5 min at room temperature. After blocking with 2.5% BSA/PBS for 30 min, aortic sections were stained with CD11c (PE, N418, eBioscience) and Mac3 (FITC, M3/84, BD) (or corresponding isotype negative controls, Supplemental Figure III) by coincubation overnight at 4°C.^{7, 8} Then the sections were washed and mounted with ProLong Gold medium (Thermo Fisher Scientific). Fluorescent images were captured by an LSM780 confocal microscope. For aortic sinus lesion detection, sections were subjected to oil red O staining. The average atherosclerotic lesion area of one slide including 8 sections from each mouse was quantified using ImageJ analysis software.

Statistics

GraphPad Prism was used for statistical analyses and figure plotting. Data are presented as mean±SEM. Student's t-test (for comparison between 2 groups) or one-way analysis of variance (for comparisons of 3 or more groups) followed by Tukey post hoc pairwise tests were used for statistical analyses of data that passed tests for the normality of distribution by Kolmogorov–Smirnov and for equal variance. If data failed normality of distribution or equal variance tests, Mann–Whitney (for 2-group comparison) or Kruskal–Wallis test (for comparison of 3 or more groups) with Dunnett post hoc pairwise test was used for statistical analyses. P<0.05 is considered statistically significant.

Results

EVOND improved lipid profiles in *Ldlr*^{-/-} mice compared to WD

After 3 months on diets, mice fed WD or EVOND gained more body weight and had larger livers and epididymal fat pads than those on ND (Figures 1A and 1B). Weight gain, food intake, and liver weights were not different between the WD and EVOND groups (Figures 1A and 1B). However, epididymal fat pad weights were lower in mice on EVOND vs. WD (Figure 1B). Consistently, body composition analysis revealed that mice fed EVOND had lower fat mass and higher lean mass than mice fed WD (Supplemental Figure IV A).

Total plasma cholesterol and TG levels were higher among mice on WD and EVOND than on ND, but were significantly lower in mice on EVOND than on WD (Figure 1C). Nevertheless, SEC analysis showed that cholesterol and TG were distributed similarly across all lipoprotein fractions in the EVOND- and WD-fed mice (Figure 1D). Similarly, hepatic TG and cholesterol content was higher in WD- vs. ND-fed mice and lower in EVOND- vs. WD-fed mice (Figure 1E). Hepatic mRNA levels of key lipogenic genes—*Srebf1*, *Scd1*, and *Fas*—and of *Cd36* were higher in mice on WD vs. ND and lower in mice on EVOND vs. WD (Figure 1F). Compared to mice fed WD, mice fed EVOND showed no significant differences in plasma glucose and insulin levels (Supplemental Figure IV B) or insulin sensitivity (Supplemental Figure IV C).

EVOND increased plasma UFA level and decreased plasma SFA level in *Ldlr*^{-/-} mice compared to WD

The plasma FA profiles of mice were drastically affected by different diets (Figures 2A and 2B). As expected, increased concentrations of several SFAs in total hydrolyzed FA and NEFA profiles were observed in mice fed WD compared to those fed ND. Palmitic acid

(C16:0) was the most abundant FA in plasma of mice fed WD, representing ~30–32% of total FA measured in total hydrolyzed FA and NEFA profiles. The percentages of palmitic acid in total hydrolyzed FA and NEFA profiles were also higher in mice on WD than on ND. In addition, the concentrations and percentages of palmitoleic acid (C16:1) and oleic acid (C18:1) were also significantly higher in the WD group than the ND group. In contrast, the percentages of most PUFAs in total hydrolyzed FA and NEFA profiles were lower in mice on WD than on ND. These changes corresponded to a dramatic decrease in the UFA/SFA ratio in the WD group compared to the ND group (Figure 2C). Compared to mice fed WD, mice fed EVOND had significant decreases in the concentrations of several SFAs, including capric acid (C10:0), lauric acid (C12:0), and myristic acid (C14:0), in total hydrolyzed FA profiles and myristic acid, palmitic acid, and stearic acid (C18:0) in NEFA profiles. The percentages of SFAs in total hydrolyzed FAs or NEFAs were mostly decreased in plasma of mice fed EVOND compared with mice fed WD. In contrast, the oleic acid level was higher in the total hydrolyzed FA profile, and palmitoleic acid was lower in total hydrolyzed FA and NEFA profiles in mice fed EVOND compared to those fed WD. Oleic acid was the major FA in plasma of EVOND-fed mice and represented ~26–28% of hydrolyzed FA and NEFA profiles. The percentages of oleic acid in total hydrolyzed FA and NEFA profiles were also or tended to be higher in mice on EVOND than on WD. Compared to mice fed WD, mice fed EVOND also had increases in the concentrations and percentages of linoleic acid (C18:2), α -linolenic acid (C18:3), and arachidonic acid (C20:4) in total hydrolyzed FA and NEFA profiles and in docosahexaenoic acid level and percentage in the total hydrolyzed FA profile.

In summary, these data show that compared to *Ldlr*^{-/-} mice fed ND, those fed WD had significantly higher plasma SFA and MUFA levels but lower plasma PUFA levels. Compared to the WD group, the EVOND group had lower plasma levels of SFA but higher levels of MUFA and PUFA. As a result, the UFA/SFA ratio was significantly higher in the EVOND group than the WD group (Figure 2C). The TBARS assay showed significantly higher plasma levels of MDA in the EVOND group than in the WD group (Supplemental Figure V), consistent with higher plasma UFA levels in the EVOND group.

EVOND suppressed FM formation and inflammation

We next examined monocyte phenotypes in the circulation and found a higher frequency of circulating monocytes in mice fed WD or EVOND than on ND, but similar frequencies in mice fed WD and EVOND (Figure 3A). The side scatter (SSC) level of monocytes, which reflects cell granularity and monocyte lipid accumulation,⁷ continuously increased over time in monocytes, indicating FM formation, in mice fed WD compared to mice fed ND (Figure 3B), in accord with our previous reports.^{7, 8} Importantly, starting within 2 months on diets, the SSC value was significantly lower, indicating less lipid accumulation, in monocytes from mice on EVOND vs. WD (Figure 3B, Supplemental Figure VI A). Nile red staining for lipids confirmed FM formation in the circulation of mice fed WD and less lipid staining in monocytes of mice on EVOND vs. WD (Figure 3B).

In contrast to our previous report showing 3 distinct monocyte subsets based on CD11c and CD36 expression, i.e., CD36⁻CD11c⁻, CD36⁺CD11c⁻, and CD36⁺CD11c⁺, in *apoE*^{-/-} mice,

⁷ our current study showed that CD36⁺CD11c⁻ and CD36⁺CD11c⁺ subsets were difficult to distinguish in *Ldlr*^{-/-} mice (Supplemental Figure I). Therefore, we classified monocytes into CD36⁻ (mainly representing Ly-6C^{high}) and CD36⁺ (mainly representing Ly-6C^{low/intermediate}) monocytes subsets in *Ldlr*^{-/-} mice (Supplemental Figure I). Compared to those in ND-fed mice, CD36⁻ monocytes in WD-fed *Ldlr*^{-/-} mice were modestly higher in SSC value. In contrast, CD36⁺ monocytes showed a dramatic increase in SSC level in *Ldlr*^{-/-} mice on WD vs. ND (Figures 3C), a finding similar to our previous report in *apoE*^{-/-} mice.⁷ Although the SSC level was not different between CD36⁺ and CD36⁻ monocytes in *Ldlr*^{-/-} mice on ND, the SSC value of CD36⁺ monocytes was significantly higher than that of CD36⁻ monocytes in mice fed WD or EVOND, consistent with our previous observations that CD36⁺ monocytes were prone to take up lipids and become FM.⁷ Of note, CD36⁺, but not CD36⁻, monocytes showed a significant decrease in SSC value, indicating less lipid accumulation, in mice fed EVOND compared with those in mice fed WD (Figures 3C).

We next examined CD11c expression on monocyte subsets. Consistent with those in *apoE*^{-/-} mice, CD36⁻ monocytes in *Ldlr*^{-/-} mice on either diet were low in CD11c expression (Figure 3D, Supplemental Figures I and VI B). In contrast, CD36⁺ monocytes were high in CD11c (Figure 3D, Supplemental Figures I and VI B). Furthermore, with the increased lipid accumulation, CD36⁺ monocytes from the WD group exhibited significantly increased CD11c MFI levels compared to those from ND group (Figure 3D), a finding similar to that in our previous report showing increased CD36⁺CD11c⁺-to-CD36⁺CD11c⁻ ratio in *apoE*^{-/-} mice fed WD. Importantly, compared to those in the WD group, CD36⁺ monocytes in the EVOND group, with less lipid accumulation, had reduced CD11c MFI levels (Figures 3D, Supplemental Figure VI B).

Lipid accumulation may increase inflammation in monocytes.^{7, 28, 29} We next examined expression of inflammatory cytokines IL-1 β and TNF α in monocytes after LPS stimulation for 4 h. Expression levels of TNF α and IL-1 β were both significantly lower in monocytes of *Ldlr*^{-/-} mice on EVOND than on WD (Figure 3E).

In summary, among *Ldlr*^{-/-} mice on EVOND vs. WD, circulating monocytes, CD36⁺ monocytes in particular, had lower lipid accumulation, which was associated with lower CD11c expression and less monocyte inflammation.

EVOND reduced monocyte uptake of oxLDL

The lower plasma levels of cholesterol and TG may contribute substantially to the altered monocyte phenotypes, including less lipid accumulation, in mice fed EVOND. Another potential contributor is the change in FA composition in plasma lipoproteins. To test this, we isolated TGRLs, which carried the majority of plasma esterified FAs, from mice fed WD and EVOND, and incubated isolated TGRLs (200 mg/dL) with monocytes from *Ldlr*^{-/-} mice on ND. Incubation of monocytes with TGRLs from mice on EVOND vs. WD was associated with lower monocyte SSC levels, indicating less lipid (Figure 4A). To determine the effects of FAs in TGRLs on monocyte phenotypes, we hydrolyzed TGRLs with LPL prior to incubation with monocytes. Similar to TGRLs, the lipolysis products (mainly FAs) of TGRLs from mice fed EVOND induced lower SSC level of monocytes than those from mice

fed WD (Supplemental Figure VII A). These findings imply that changes in FA composition may alter TGRL-mediated effects on monocyte lipid accumulation.

Lipid accumulation in monocytes also increased CD36 levels as indicated by mean fluorescence intensity.⁷ Along with reduced lipid accumulation, monocytes in mice fed EVOND expressed lower level of CD36 than those fed WD (Figure 4B). Consistent with less lipid accumulation, monocytes treated ex vivo with TGRLs from EVOND-fed mice also had or tended to have lower CD36 levels than monocytes treated with TGRLs from WD-fed mice (Figure 4C, Supplemental Figure VII B).

While TGRLs contribute to monocyte foam cell formation, LDL, particularly modified LDL such as oxLDL, is the major lipoprotein that causes foam cell formation in atherosclerotic lesions.^{30, 31} Monocyte/macrophage uptake of modified LDL is a key step in atherosclerotic foam cell formation, in which CD36 plays an important role.^{7, 11, 32} Therefore, we tested whether the differences in monocyte levels of CD36 between WD and EVOND groups affected monocyte uptake of oxLDL and observed that after ex vivo incubation with DiI-oxLDL, monocytes in mice fed EVOND had significantly lower DiI levels, indicating less oxLDL uptake, than those in mice fed WD (Figure 4C). Furthermore, blocking of CD36 with an antibody significantly decreased monocyte uptake of oxLDL. These data indicated that reductions in monocyte levels of CD36 in mice fed EVOND were associated with less monocyte uptake of modified LDL, which may also contribute to reductions in monocyte lipid accumulation and foam cell formation in these mice.

EVOND reduced FM adhesion

CD11c, a $\beta 2$ integrin upregulated on monocytes with lipid accumulation (FM formation) in hyperlipidemia,^{7, 8} mediates monocyte adhesion to endothelial cells,^{33, 34} a process important for inflammation including atherosclerosis. Indeed, we have previously shown that CD11c on monocytes contributes to the development of atherosclerosis.^{7, 8} Consistently, compared to those in mice on ND, monocytes in mice fed WD, with lipid accumulation (FM formation) and increased CD11c expression (Figures 3B and 3D), had enhanced adhesion to VCAM-1 and E-selectin, indicated by increased frequencies of firmly arrested CD11c⁺ monocytes on these endothelial adhesion molecules in the ex vivo flow adhesion assay (Figures 5A and 5B). In contrast, monocytes in mice fed EVOND, with less lipid accumulation and reduced CD11c expression (Figures 3B and 3D), had significantly reduced adhesion to VCAM-1 and E-selectin compared to those from mice fed WD (Figures 5A and 5B).

EVOND reduced atherosclerosis development

Finally, we examined effects of EVOND on development of atherosclerosis in *Ldlr*^{-/-} mice. Oil red O staining showed that mice on ND had minor atherosclerotic lesions and that mice fed WD for 3 months developed profound atherosclerosis in the whole aorta and aortic sinus (Figure 6A). Along with the above changes in monocyte phenotypes and plasma lipid levels, mice fed EVOND developed significantly less atherosclerosis in whole aorta and aortic sinus compared to mice fed WD (Figures 6A and 6B). A separate set of experiments showed that mice on EVOND vs. WD for 6 months had greater reductions in development of

atherosclerosis (34.2% reduction, Supplemental Figures VIII A and VIII B) than those on diets for 3 months (25.6% reduction). Further analyses of lesion formation in different locations in the aorta showed that mice fed EVOND as compared to WD displayed significantly smaller lesions in aortic arch and descending aortic regions (Supplemental Figures IX A and IX B). With reduced FM (CD11c⁺) adhesion, mice fed EVOND also had significantly less CD11c⁺ macrophage/dendritic cell accumulation in atherosclerotic lesions compared to mice fed WD (Figures 6C and 6D).

Discussion

Different types of dietary fat may play distinct roles in cardiovascular health.^{35–37} The clinical outcomes of the PREDIMED, REDUCE-IT, and CANTOS trials have increased the priority of understanding how dietary FAs impact atherosclerosis, lipoproteins, and inflammation.^{1, 4, 38} Our current study showed that replacement of SFA from milkfat with UFA from extra-virgin olive oil and nuts in a cholesterol-rich WD reduced development of atherosclerosis in *Ldlr*^{-/-} mice, in support of the clinical benefits of Mediterranean-type diet supplemented with extra-virgin olive oil and nuts in reducing the risk for cardiovascular events as demonstrated by the PREDIMED clinical trial.¹ The decreased plasma lipid concentrations with EVOND may play an important role in the reduced atherosclerosis. However, how changes in plasma lipid concentrations alter atherogenesis remains incompletely understood. We made the novel observations that compared to WD, EVOND improved circulating monocyte phenotypes, with reductions in monocyte lipid accumulation, inflammation, expression of CD36 and CD11c, oxLDL uptake, and monocyte adhesion capacity, in this mouse model of atherosclerosis. Given the recent CANTOS study showing the benefits of targeting inflammation for prevention of atherosclerotic cardiovascular disease events,³⁹ our observations of improved monocyte inflammatory phenotypes, which can be induced by reduced plasma lipid concentrations and altered FA composition (see the following discussion), may provide an important mechanism underlying the protective effect of EVOND on atherogenesis.

Compared to WD, EVOND is high in UFAs, including MUFAs and PUFAs, but low in SFAs. As expected, plasma levels of UFAs were higher and of SFAs were lower in mice fed EVOND than in mice fed WD. Specifically, compared to mice fed WD, mice fed EVOND had higher plasma levels of oleic acid and linoleic acid and lower levels of capric acid, lauric acid, and myristic acid, which reflected the differences in abundance of these FAs between EVOND and WD. In addition, mice fed EVOND compared to WD also had higher plasma levels of α -linolenic acid, arachidonic acid, and DHA, which were different from the content of these FAs in each diet. Furthermore, our study showed smaller changes in FA profiles in mouse plasma than in diets. This may be because of the role of hepatic de novo FA synthesis and other mechanisms such as lipolysis in adipose tissue and fat utilization in muscle in response to different dietary fats. Importantly, compared to WD, EVOND reduced plasma and hepatic levels of cholesterol and TG in *Ldlr*^{-/-} mice. Previous studies have demonstrated that high UFA intake reduced plasma and hepatic levels of cholesterol and TG through regulating lipid metabolism.^{40–43} In contrast, SFAs have been shown to promote lipid biosynthesis in the liver, leading to increases in hepatic and plasma lipid levels.^{44, 45} Consistent with these reports, we observed that hepatic expression of lipogenic genes was

decreased in EVOND-fed mice compared to WD-fed mice, suggesting that a diet high in UFAs (i.e., EVOND) has a favorable impact on the plasma lipid profile and hepatic lipid metabolism compared to a diet high in SFAs (i.e., WD).

Elevated plasma levels of cholesterol and TG transported in lipoproteins play important roles in monocyte uptake of lipids, resulting in formation of FM.^{7, 8, 13, 34, 46, 47} Therefore, decreased plasma levels of TG and cholesterol in mice fed EVOND may lead to less monocyte lipid accumulation and reduced FM formation. Consistently, reduction of hyperlipidemia in humans with familial hypercholesterolemia decreases lipid accumulation within circulating monocytes.^{6, 12} Beyond the effect of blood cholesterol and TG levels, we observed that lipid accumulation in monocytes was reduced by treatment with TGRLs from EVOND-fed mice compared to those from WD-fed mice at the same TG concentration, also supporting a role for altered lipoprotein FA composition in monocyte uptake of TGRLs and FM formation. Our ongoing and future studies will examine the mechanisms by which monocytes take up TGRLs.

Lipid accumulation may upregulate proinflammatory marker expression in monocytes/macrophages.^{7, 28, 29} Therefore, less lipid accumulation in monocytes of mice fed EVOND may contribute to decreased monocyte inflammation in these mice. In addition, SFAs, but not UFAs, induce expression of inflammatory cytokines in monocytes.^{48, 49} Therefore, the changes in FA profiles may also contribute to reduced monocyte inflammation in mice fed EVOND.

While TG and FAs contribute to lipid accumulation within monocytes,^{13, 46, 47, 50} the major lipoprotein that induces foam cell formation for atherosclerosis is LDL, and oxLDL is believed to be a particularly potent substrate for this process.⁵¹ CD36, a type of scavenger receptor class B, plays a crucial role in monocyte/macrophage uptake of modified LDL and FM formation.^{7, 29, 52} In turn, lipid accumulation in monocytes further increases expression of CD36, forming a positive feedback loop to accelerate FM formation. Indeed, our current and previous studies showed preferential FM formation of CD36⁺ monocytes and further upregulation of CD36 on FM in mice fed WD.⁷ The lower CD36 levels on monocytes in mice on EVOND than on WD may also be caused by less lipid accumulation and the changes in FA composition within monocytes, as indicated by our ex vivo TGRL treatment assay. Indeed, palmitate, the most abundant SFA in WD and in plasma of WD-fed mice, upregulates CD36 expression on monocytes/macrophages.⁵³ Importantly, the reduction in monocyte CD36 levels in mice fed EVOND was associated with reduced monocyte uptake of oxLDL, which may, in turn, contribute (at least partially) to the reduced monocyte lipid accumulation and foam cell formation and to decreased atherosclerosis in these mice fed EVOND. These data indicate that the changes in dietary fat composition by replacement of SFAs with UFAs result in lower monocyte CD36 expression, and therefore likely reduce monocyte lipid accumulation, foam cell formation, and inflammation. Our future approach will also need to examine additional mechanisms for monocyte uptake of oxLDL and lipid accumulation.

Lipid accumulation also increases monocyte/macrophage expression of CD11c, which mediates monocyte adhesion on endothelial cells and transendothelial migration into arterial

walls.^{7, 30} While many previous investigations showed that MUFA and PUFA infusion or dietary supplementation reduced monocyte endothelium adhesion in humans and animals,^{54, 55} the mechanisms underlying reduced monocyte adhesion remain poorly understood. Our current study provides evidence supporting the hypothesis that less monocyte lipid accumulation leading to lower monocyte expression of CD11c may underlie the reduced monocyte adhesion to endothelial cells in mice on high-UFA diet. Reduction of monocyte CD11c and adhesion may also underlie the reduced accumulation of CD11c⁺ macrophages/dendritic cells in atherosclerotic plaques and decreased atherosclerosis development in mice fed EVOND.

In our current study, we examined effects of changing the dietary FA composition by replacing milkfat with extra-virgin olive oil and mixed nuts in WD on monocyte phenotypes and atherosclerosis. However, some limitations should be noted. First, only male mice were studied. Considering that sex is an important biological variable, our future study will consider to compare male and female mice side-by-side. Second, we were not able to identify the specific FAs that may play a major role in the underlying pathophysiologic pathways discovered in our study. However, diet intake studies using high concentrations of highly purified FAs would be cost prohibitive and less relevant to human clinical studies. Third, the current study did not test the FA composition in plasma triglycerides and cholesteryl esters. Fourth, because of concerns in regard to limitations of commercial reagents for murine studies, we did not measure plasma levels of oxLDL in these mice. Instead, we analyzed plasma MDA level and found that higher plasma MDA levels in mice fed EVOND were consistent with the higher plasma UFA levels in these mice. Fifth, because of difficulty in obtaining sufficient monocytes from mouse blood, we were unable to perform intercellular FA profiling and gene network analysis (as shown in macrophages of *Ldlr*^{-/-} mice on WD⁵⁶) in foamy monocytes.

Our study in mice provides important mechanistic views as to how changes in dietary FA composition may impact monocyte phenotypes and atherosclerosis. The most recent results of the REDUCE-IT study, in which the addition of highly purified EPA led to reduced risk of ischemic events greater than predicted on the basis of the changes in plasma TG levels in patients with hypertriglyceridemia, suggest that other mechanisms beyond plasma lipid-lowering effects played a role in reduction of atherosclerotic events by EPA.^{38, 57} We have previously shown that EPA improved fasting and postprandial monocyte phenotypes with reduced CD11c and CD36 levels on monocytes, with no significant reductions in postprandial blood TG levels, in subjects with hypertriglyceridemia,⁴⁷ supporting a potential important role of improvements of monocyte phenotypes in reducing cardiovascular risk.

In summary, our current study showed that compared to WD high in SFAs, EVOND with high UFAs but low SFAs reduced FM formation, with decreased monocyte inflammation, lipid uptake, and adhesion, and decelerated atherosclerosis development in *Ldlr*^{-/-} mice, thereby highlighting an important role of changes in dietary fat composition in regulating monocyte phenotypes and atherosclerosis.

Supplementary Material

Refer to Web version on PubMed Central for supplementary material.

Acknowledgments

We thank Kerrie Jara for editorial assistance.

Sources of Funding

This work was supported by NIH grants under Award Numbers R01 HL098839 (HW), R01 AI047294 (SIS), R01 HL082689 (SIS) and R01 HL056865 (HJP), an American Heart Association Award AHA16GRNT30410012, and an American Diabetes Association Award 1-17-IBS-082 (HW).

Nonstandard Abbreviations and Acronyms

EVOND	extra-virgin olive oil and nuts diet
FA	fatty acid
FM	foamy monocyte
<i>Ldlr</i>^{-/-}	low-density lipoprotein receptor knockout
MUFA	monounsaturated fatty acid
ND	normal diet
NEFA	nonesterified fatty acid
oxLDL	oxidized low-density lipoprotein
PUFA	polyunsaturated fatty acid
SFA	saturated fatty acid
SSC	side scatter
TG	triglyceride
TGRL	triglyceride-rich lipoprotein
UFA	unsaturated fatty acid
WD	western diet

References

1. Estruch R, Ros E, Salas-Salvado J, Covas MI, Corella D, Aros F, Gomez-Gracia E, Ruiz-Gutierrez V, Fiol M, Lapetra J, Lamuela-Raventos RM, Serra-Majem L, Pinto X, Basora J, Munoz MA, Sorli JV, Martinez JA, Fito M, Gea A, Hernan MA, Martinez-Gonzalez MA and Investigators PS. Primary Prevention of Cardiovascular Disease with a Mediterranean Diet Supplemented with Extra-Virgin Olive Oil or Nuts. *N Engl J Med.* 2018;378:e34. [PubMed: 29897866]
2. Sacks FM, Lichtenstein AH, Wu JHY, Appel LJ, Creager MA, Kris-Etherton PM, Miller M, Rimm EB, Rudel LL, Robinson JG, Stone NJ, Van Horn LV and American Heart A. Dietary Fats and

Cardiovascular Disease: A Presidential Advisory From the American Heart Association. *Circulation*. 2017;136:e1–e23. [PubMed: 28620111]

3. Chowdhury R, Warnakula S, Kunutsor S, Crowe F, Ward HA, Johnson L, Franco OH, Butterworth AS, Forouhi NG, Thompson SG, Khaw KT, Mozaffarian D, Danesh J and Di Angelantonio E. Association of dietary, circulating, and supplement fatty acids with coronary risk: a systematic review and meta-analysis. *Ann Intern Med*. 2014;160:398–406. [PubMed: 24723079]
4. Ridker PM, Everett BM, Thuren T, MacFadyen JG, Chang WH, Ballantyne C, Fonseca F, Nicolau J, Koenig W, Anker SD, Kastelein JJP, Cornel JH, Pais P, Pella D, Genest J, Cifkova R, Lorenzatti A, Forster T, Kobalava Z, Vida-Simiti L, Flather M, Shimokawa H, Ogawa H, Dellborg M, Rossi PRF, Troquay RPT, Libby P, Glynn RJ and Group CT. Antiinflammatory Therapy with Canakinumab for Atherosclerotic Disease. *N Engl J Med*. 2017;377:1119–1131. [PubMed: 28845751]
5. Tabas I and Bornfeldt KE. Macrophage Phenotype and Function in Different Stages of Atherosclerosis. *Circ Res*. 2016;118:653–667. [PubMed: 26892964]
6. Wu H and Ballantyne CM. Dyslipidaemia: PCSK9 inhibitors and foamy monocytes in familial hypercholesterolaemia. *Nat Rev Cardiol*. 2017;14:385–386. [PubMed: 28492287]
7. Xu L, Dai Perrard X, Perrard JL, Yang D, Xiao X, Teng BB, Simon SI, Ballantyne CM and Wu H. Foamy monocytes form early and contribute to nascent atherosclerosis in mice with hypercholesterolemia. *Arterioscler Thromb Vasc Biol*. 2015;35:1787–1797. [PubMed: 26112011]
8. Wu H, Gower RM, Wang H, Perrard XY, Ma R, Bullard DC, Burns AR, Paul A, Smith CW, Simon SI and Ballantyne CM. Functional role of CD11c+ monocytes in atherogenesis associated with hypercholesterolemia. *Circulation*. 2009;119:2708–2717. [PubMed: 19433759]
9. Ley K, Miller YI and Hedrick CC. Monocyte and macrophage dynamics during atherogenesis. *Arterioscler Thromb Vasc Biol*. 2011;31:1506–1516. [PubMed: 21677293]
10. Tacke F, Alvarez D, Kaplan TJ, Jakubzick C, Spanbroek R, Llodra J, Garin A, Liu J, Mack M, van Rooijen N, Lira SA, Habenicht AJ and Randolph GJ. Monocyte subsets differentially employ CCR2, CCR5, and CX3CR1 to accumulate within atherosclerotic plaques. *J Clin Invest*. 2007;117:185–194. [PubMed: 17200718]
11. Joffe J, Potteaux S, Zeboudj L, Loyer X, Boufenzar A, Laurans L, Esposito B, Vandestienne M, de Jager SC, Henique C, Zlatanova I, Taleb S, Bruneval P, Tedgui A, Mallat Z, Gibot S and Ait-Oufella H. Genetic and Pharmacological Inhibition of TREM-1 Limits the Development of Experimental Atherosclerosis. *J Am Coll Cardiol*. 2016;68:2776–2793. [PubMed: 28007141]
12. Bernelot Moens SJ, Neele AE, Kroon J, van der Valk FM, Van den Bossche J, Hoeksema MA, Hoogeveen RM, Schnitzler JG, Baccara-Dinet MT, Manvelian G, de Winther MPJ and Stroes ESG. PCSK9 monoclonal antibodies reverse the pro-inflammatory profile of monocytes in familial hypercholesterolaemia. *Eur Heart J*. 2017;38:1584–1593. [PubMed: 28329114]
13. Khan IM, Pokharel Y, Dadu RT, Lewis DE, Hoogeveen RC, Wu H and Ballantyne CM. Postprandial Monocyte Activation in Individuals With Metabolic Syndrome. *J Clin Endocrinol Metab*. 2016;101:4195–4204. [PubMed: 27575945]
14. Robinet P, Milewicz DM, Cassis LA, Leeper NJ, Lu HS and Smith JD. Consideration of Sex Differences in Design and Reporting of Experimental Arterial Pathology Studies-Statement From ATV Council. *Arterioscler Thromb Vasc Biol*. 2018;38:292–303. [PubMed: 29301789]
15. Bourassa PA, Milos PM, Gaynor BJ, Breslow JL and Aiello RJ. Estrogen reduces atherosclerotic lesion development in apolipoprotein E-deficient mice. *Proc Natl Acad Sci U S A*. 1996;93:10022–10027. [PubMed: 8816744]
16. Wu C, Daugherty A and Lu HS. Updates on Approaches for Studying Atherosclerosis. *Arterioscler Thromb Vasc Biol*. 2019;39:e108–e117. [PubMed: 30917052]
17. Khan IM, Dai Perrard XY, Perrard JL, Mansoori A, Smith CW, Wu H and Ballantyne CM. Attenuated adipose tissue and skeletal muscle inflammation in obese mice with combined CD4+ and CD8+ T cell deficiency. *Atherosclerosis*. 2014;233:419–428. [PubMed: 24530773]
18. Lepage G and Roy CC. Specific methylation of plasma nonesterified fatty acids in a one-step reaction. *J Lipid Res*. 1988;29:227–235. [PubMed: 3367090]
19. Wang Q, Perrard XD, Perrard JL, Mansoori A, Raya JL, Hoogeveen R, Smith CW, Ballantyne CM and Wu H. Differential effect of weight loss with low-fat diet or high-fat diet restriction on

- inflammation in the liver and adipose tissue of mice with diet-induced obesity. *Atherosclerosis*. 2011;219:100–108. [PubMed: 21824616]
20. Rosales C, Tang D, Gillard BK, Courtney HS and Pownall HJ. Apolipoprotein E mediates enhanced plasma high-density lipoprotein cholesterol clearance by low-dose streptococcal serum opacity factor via hepatic low-density lipoprotein receptors in vivo. *Arterioscler Thromb Vasc Biol*. 2011;31:1834–1841. [PubMed: 21597008]
 21. Wang X and Seed B. A PCR primer bank for quantitative gene expression analysis. *Nucleic Acids Res*. 2003;31:e154. [PubMed: 14654707]
 22. Zhang D, Fang P, Jiang X, Nelson J, Moore JK, Kruger WD, Berretta RM, Houser SR, Yang X and Wang H. Severe hyperhomocysteinemia promotes bone marrow-derived and resident inflammatory monocyte differentiation and atherosclerosis in LDLr/CBS-deficient mice. *Circ Res*. 2012;111:37–49. [PubMed: 22628578]
 23. Eiselein L, Wilson DW, Lame MW and Rutledge JC. Lipolysis products from triglyceride-rich lipoproteins increase endothelial permeability, perturb zonula occludens-1 and F-actin, and induce apoptosis. *Am J Physiol Heart Circ Physiol*. 2007;292:H2745–2753. [PubMed: 17259442]
 24. Foster GA, Gower RM, Stanhope KL, Havel PJ, Simon SI and Armstrong EJ. On-chip phenotypic analysis of inflammatory monocytes in atherogenesis and myocardial infarction. *Proc Natl Acad Sci U S A*. 2013;110:13944–13949. [PubMed: 23918401]
 25. Wang H, Jiang X, Yang F, Gaubatz JW, Ma L, Magera MJ, Yang X, Berger PB, Durante W, Pownall HJ and Schafer AI. Hyperhomocysteinemia accelerates atherosclerosis in cystathionine beta-synthase and apolipoprotein E double knock-out mice with and without dietary perturbation. *Blood*. 2003;101:3901–3907. [PubMed: 12506016]
 26. Croce K, Gao H, Wang Y, Mooroka T, Sakuma M, Shi C, Sukhova GK, Packard RR, Hogg N, Libby P and Simon DI. Myeloid-related protein-8/14 is critical for the biological response to vascular injury. *Circulation*. 2009;120:427–436. [PubMed: 19620505]
 27. Daugherty A, Tall AR, Daemen M, Falk E, Fisher EA, Garcia-Cardena G, Lusis AJ, Owens AP 3rd, Rosenfeld ME, Virmani R, American Heart Association Council on Arteriosclerosis T, Vascular B and Council on Basic Cardiovascular S. Recommendation on Design, Execution, and Reporting of Animal Atherosclerosis Studies: A Scientific Statement From the American Heart Association. *Arterioscler Thromb Vasc Biol*. 2017;37:e131–e157. [PubMed: 28729366]
 28. Koelwyn GJ, Corr EM, Erbay E and Moore KJ. Regulation of macrophage immunometabolism in atherosclerosis. *Nat Immunol*. 2018;19:526–537. [PubMed: 29777212]
 29. Bekkering S, Quintin J, Joosten LA, van der Meer JW, Netea MG and Riksen NP. Oxidized low-density lipoprotein induces long-term proinflammatory cytokine production and foam cell formation via epigenetic reprogramming of monocytes. *Arterioscler Thromb Vasc Biol*. 2014;34:1731–1738. [PubMed: 24903093]
 30. Cho HJ, Shashkin P, Gleissner CA, Dunson D, Jain N, Lee JK, Miller Y and Ley K. Induction of dendritic cell-like phenotype in macrophages during foam cell formation. *Physiol Genomics*. 2007;29:149–160. [PubMed: 17244792]
 31. Febbraio M, Podrez EA, Smith JD, Hajjar DP, Hazen SL, Hoff HF, Sharma K and Silverstein RL. Targeted disruption of the class B scavenger receptor CD36 protects against atherosclerotic lesion development in mice. *J Clin Invest*. 2000;105:1049–1056. [PubMed: 10772649]
 32. Thomas GD, Hamers AAJ, Nakao C, Marcovecchio P, Taylor AM, McSkimming C, Nguyen AT, McNamara CA and Hedrick CC. Human Blood Monocyte Subsets: A New Gating Strategy Defined Using Cell Surface Markers Identified by Mass Cytometry. *Arterioscler Thromb Vasc Biol*. 2017;37:1548–1558. [PubMed: 28596372]
 33. Uotila LM, Aatonen M and Gahmberg CG. Integrin CD11c/CD18 alpha-chain phosphorylation is functionally important. *J Biol Chem*. 2013;288:33494–33499. [PubMed: 24129562]
 34. Foster GA, Xu L, Chidambaram AA, Soderberg SR, Armstrong EJ, Wu H and Simon SI. CD11c/CD18 Signals Very Late Antigen-4 Activation To Initiate Foamy Monocyte Recruitment during the Onset of Hypercholesterolemia. *J Immunol*. 2015;195:5380–5392. [PubMed: 26519532]
 35. Watts GF, Lewis B, Brunt JN, Lewis ES, Coltart DJ, Smith LD, Mann JI and Swan AV. Effects on coronary artery disease of lipid-lowering diet, or diet plus cholestyramine, in the St Thomas' Atherosclerosis Regression Study (STARS). *Lancet*. 1992;339:563–569. [PubMed: 1347091]

36. Hernaez A, Castaner O, Elosua R, Pinto X, Estruch R, Salas-Salvado J, Corella D, Aros F, Serra-Majem L, Fiol M, Ortega-Calvo M, Ros E, Martinez-Gonzalez MA, de la Torre R, Lopez-Sabater MC and Fito M. Mediterranean Diet Improves High-Density Lipoprotein Function in High-Cardiovascular-Risk Individuals: A Randomized Controlled Trial. *Circulation*. 2017;135:633–643. [PubMed: 28193797]
37. Getz GS and Reardon CA. Diet and murine atherosclerosis. *Arterioscler Thromb Vasc Biol*. 2006;26:242–249. [PubMed: 16373607]
38. Bhatt DL, Steg PG, Miller M, Brinton EA, Jacobson TA, Ketchum SB, Doyle RT Jr., Juliano RA, Jiao L, Granowitz C, Tardif JC, Ballantyne CM and Investigators R-I. Cardiovascular Risk Reduction with Icosapent Ethyl for Hypertriglyceridemia. *N Engl J Med*. 2018.
39. Weber C and von Hundelshausen P. CANTOS Trial Validates the Inflammatory Pathogenesis of Atherosclerosis: Setting the Stage for a New Chapter in Therapeutic Targeting. *Circ Res*. 2017;121:1119–1121. [PubMed: 29074528]
40. Vasandani C, Kafrouni AI, Caronna A, Bashmakov Y, Gotthardt M, Horton JD and Spady DK. Upregulation of hepatic LDL transport by n-3 fatty acids in LDL receptor knockout mice. *J Lipid Res*. 2002;43:772–784. [PubMed: 11971949]
41. Jurado-Ruiz E, Varela LM, Luque A, Berna G, Cahuana G, Martinez-Force E, Gallego-Duran R, Soria B, de Roos B, Romero Gomez M and Martin F. An extra virgin olive oil rich diet intervention ameliorates the nonalcoholic steatohepatitis induced by a high-fat “Western-type” diet in mice. *Mol Nutr Food Res*. 2017;61.
42. Wang S, Matthan NR, Wu D, Reed DB, Bapat P, Yin X, Grammas P, Shen CL and Lichtenstein AH. Lipid content in hepatic and gonadal adipose tissue parallel aortic cholesterol accumulation in mice fed diets with different omega-6 PUFA to EPA plus DHA ratios. *Clin Nutr*. 2014;33:260–266. [PubMed: 23672804]
43. Vijaimohan K, Jainu M, Sabitha KE, Subramaniam S, Anandhan C and Shyamala Devi CS. Beneficial effects of alpha linolenic acid rich flaxseed oil on growth performance and hepatic cholesterol metabolism in high fat diet fed rats. *Life Sci*. 2006;79:448–454. [PubMed: 16490217]
44. Fernandez ML and West KL. Mechanisms by which dietary fatty acids modulate plasma lipids. *J Nutr*. 2005;135:2075–2078. [PubMed: 16140878]
45. Lin J, Yang R, Tarr PT, Wu PH, Handschin C, Li S, Yang W, Pei L, Uldry M, Tontonoz P, Newgard CB and Spiegelman BM. Hyperlipidemic effects of dietary saturated fats mediated through PGC-1beta coactivation of SREBP. *Cell*. 2005;120:261–273. [PubMed: 15680331]
46. Gower RM, Wu H, Foster GA, Devaraj S, Jialal I, Ballantyne CM, Knowlton AA and Simon SI. CD11c/CD18 expression is upregulated on blood monocytes during hypertriglyceridemia and enhances adhesion to vascular cell adhesion molecule-1. *Arterioscler Thromb Vasc Biol*. 2011;31:160–166. [PubMed: 21030716]
47. Dai Perrard XY, Lian Z, Bobotas G, Dicklin MR, Maki KC and Wu H. Effects of n-3 fatty acid treatment on monocyte phenotypes in humans with hypertriglyceridemia. *J Clin Lipidol*. 2017;11:1361–1371. [PubMed: 28942094]
48. Pillon NJ, Chan KL, Zhang S, Mejdani M, Jacobson MR, Ducos A, Bilan PJ, Niu W and Klip A. Saturated fatty acids activate caspase-4/5 in human monocytes, triggering IL-1beta and IL-18 release. *Am J Physiol Endocrinol Metab*. 2016;311:E825–E835. [PubMed: 27624102]
49. Singh V, Rana M, Jain M, Singh N, Naqvi A, Malasoni R, Dwivedi AK, Dikshit M and Barthwal MK. Curcuma oil attenuates accelerated atherosclerosis and macrophage foam-cell formation by modulating genes involved in plaque stability, lipid homeostasis and inflammation. *Br J Nutr*. 2015;113:100–113. [PubMed: 25391643]
50. den Hartigh LJ, Connolly-Rohrbach JE, Fore S, Huser TR and Rutledge JC. Fatty acids from very low-density lipoprotein lipolysis products induce lipid droplet accumulation in human monocytes. *J Immunol*. 2010;184:3927–3936. [PubMed: 20208007]
51. Glass CK and Witztum JL. Atherosclerosis. the road ahead. *Cell*. 2001;104:503–516. [PubMed: 11239408]
52. Febbraio M, Hajjar DP and Silverstein RL. CD36: a class B scavenger receptor involved in angiogenesis, atherosclerosis, inflammation, and lipid metabolism. *J Clin Invest*. 2001;108:785–791. [PubMed: 11560944]

53. Lu Z, Li Y, Brinson CW, Kirkwood KL, Lopes-Virella MF and Huang Y. CD36 is upregulated in mice with periodontitis and metabolic syndrome and involved in macrophage gene upregulation by palmitate. *Oral Dis.* 2017;23:210–218. [PubMed: 27753178]
54. Calder PC, Bond JA, Harvey DJ, Gordon S and Newsholme EA. Uptake and incorporation of saturated and unsaturated fatty acids into macrophage lipids and their effect upon macrophage adhesion and phagocytosis. *Biochem J.* 1990;269:807–814. [PubMed: 2117922]
55. Baumann KH, Hessel F, Larass I, Muller T, Angerer P, Kiefl R and von Schacky C. Dietary omega-3, omega-6, and omega-9 unsaturated fatty acids and growth factor and cytokine gene expression in unstimulated and stimulated monocytes. A randomized volunteer study. *Arterioscler Thromb Vasc Biol.* 1999;19:59–66. [PubMed: 9888867]
56. Becker L, Gharib SA, Irwin AD, Wijsman E, Vaisar T, Oram JF and Heinecke JW. A macrophage sterol-responsive network linked to atherogenesis. *Cell Metab.* 2010;11:125–135. [PubMed: 20142100]
57. Kastelein JJP and Stroes ESG. FISHing for the Miracle of Eicosapentaenoic Acid. *N Engl J Med.* 2018.

Highlights

1. Extra-virgin olive oil and nuts diet lowered plasma lipid elevations compared with western diet in *Ldlr*^{-/-} mice
2. Compared to western diet, extra-virgin olive oil and nuts diet decreased foamy monocyte formation and inflammation.
3. Extra-virgin olive oil and nuts diet decreased CD11c expression and adhesive capacity of monocytes.
4. Extra-virgin olive oil and nuts diet reduced atherosclerotic lesion size compared to western diet.

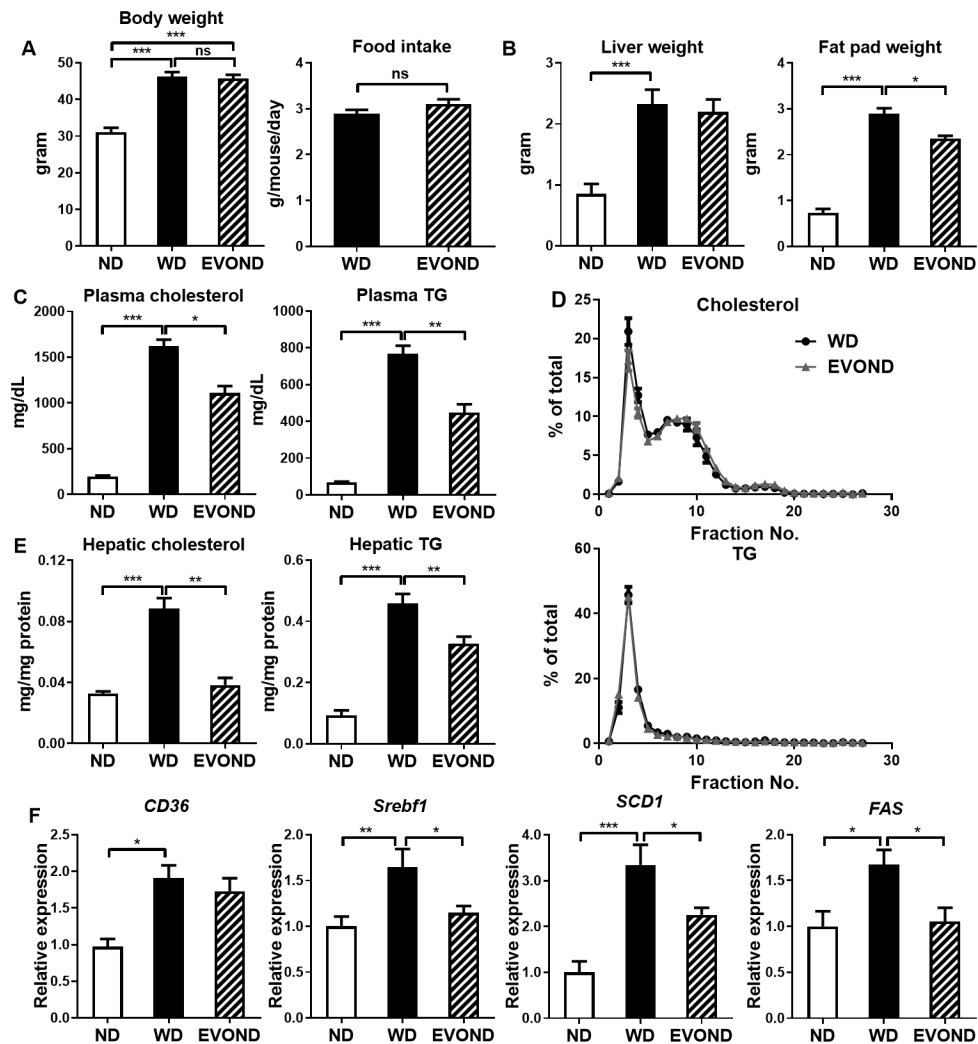
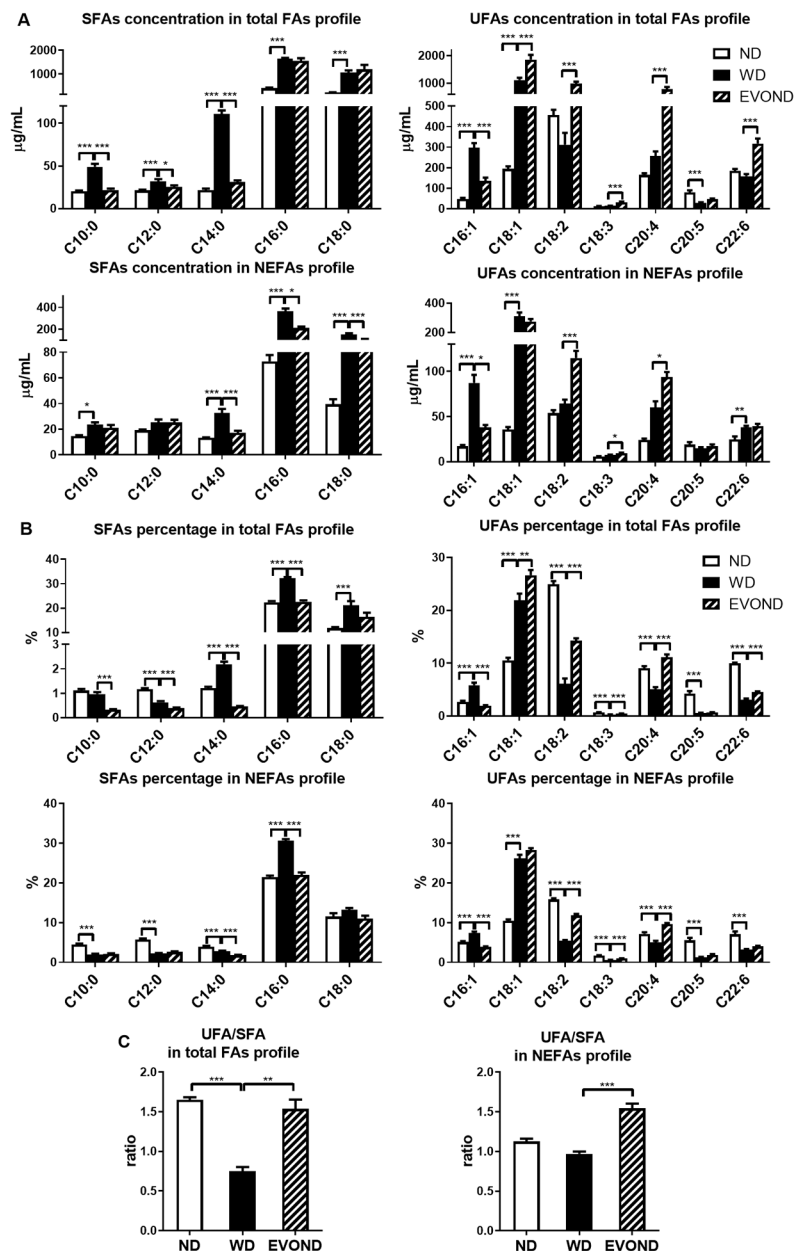
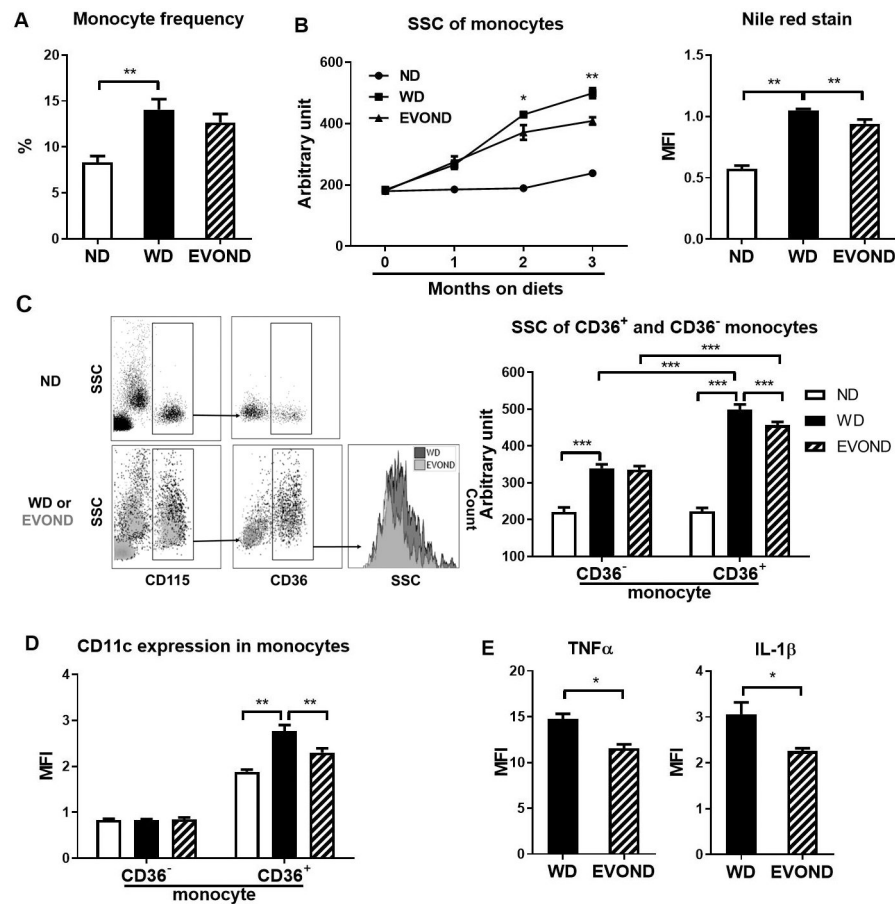


Figure 1.

In low-density lipoprotein receptor–knockout (*Ldlr*^{-/-}) mice, extra-virgin olive oil and nuts diet (EVOND) improved lipid profiles compared to western diet (WD). Eight-week-old male *Ldlr*^{-/-} mice were fed normal laboratory diet (ND), WD, or EVOND for 3 months. A, Body weight (n=12–20/group) and average food intake (n=5/group). B, Liver and epididymal fat pad weight (n=12–20/group). C, Fasting plasma total cholesterol and triglyceride (TG) levels (n=12–20/group). D, Plasma lipoprotein profile from mice on WD or EVOND showing cholesterol and TG distribution in each lipoprotein fraction (n=7/group). E, Hepatic TG and cholesterol content (n=9–13/group). F, mRNA levels of lipogenic genes in the liver (n=9–12/group). Data are presented as mean±SEM. *p<0.05, **p<0.01, ***p<0.001; ns, not significant.

**Figure 2.**

Plasma fatty acid (FA) profiles showed higher unsaturated fatty acid (UFA) and lower saturated fatty acid (SFA) concentrations in mice on EVOND than on WD. A, Concentrations of each SFA and UFA in total hydrolyzed FA profiles or nonesterified fatty acid (NEFA) profiles. B, Percentages of each SFA and UFA in total hydrolyzed FA profiles or NEFA profiles. C, UFA/SFA ratio in total hydrolyzed FA profiles or NEFA profiles. Data are shown as mean±SEM (n=9–12/group); *p<0.05, **p<0.01, ***p<0.001.

**Figure 3.**

EVOND compared to WD reduced foamy monocyte formation and inflammation in *Ldlr*^{-/-} mice. A, Monocyte frequency in total leukocytes of mice on ND, WD, and EVOND (n=12–20/group). B, Side scatter (SSC) value and Nile red mean fluorescence intensity (MFI) of circulating monocytes of mice on different diets (3 months on diets for Nile red staining). C, Representative fluorescence-activated cell sorter (FACS) examples showing foamy monocytes in blood of *Ldlr*^{-/-} mice on different diets (left panel). Monocytes (CD115⁺) were divided into two subsets based on CD36. Elevations in SSC indicated lipid accumulation and foamy monocyte formation; quantification of SSC values of CD36⁻ and CD36⁺ monocytes in *Ldlr*^{-/-} mice on diets (n=9–18/group; right panel). D, CD11c expression on CD36⁻ and CD36⁺ monocytes in *Ldlr*^{-/-} mice on diets (n=9–18/group). E, Expression of TNF α and IL-1 β in monocytes of *Ldlr*^{-/-} mice on diets (n=4/group). Data are shown as mean \pm SEM. *p<0.05, **p<0.01, ***p<0.001.

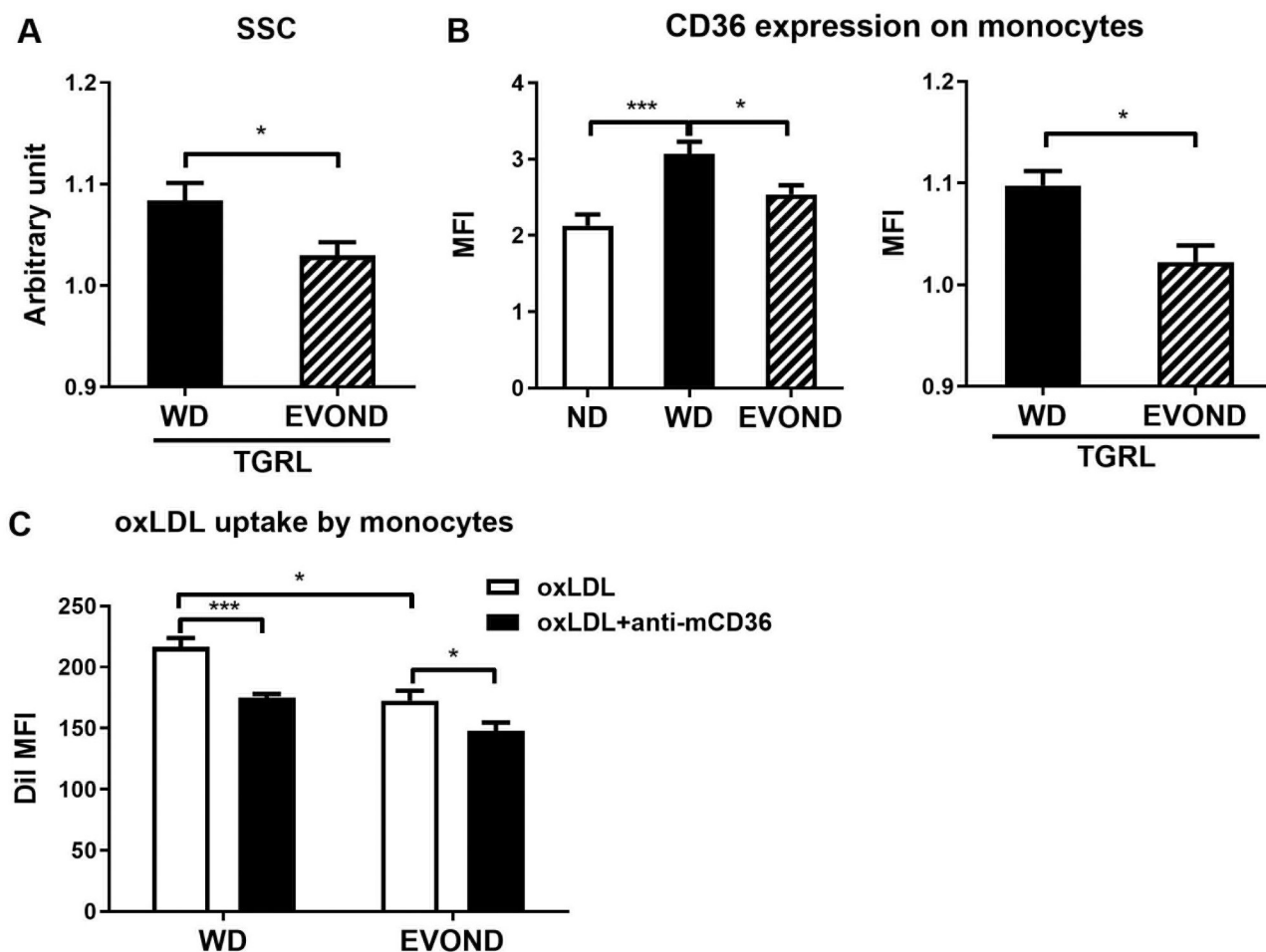


Figure 4.

EVOND reduced monocyte CD36 expression and oxidized LDL (oxLDL) uptake. A, SSC value of monocytes (from ND-fed *Ldlr*^{-/-} mice) after incubation with triglyceride-rich lipoprotein (TGRL) fraction from mice on WD or EVOND (n=6/group). B, Expression level of CD36 on circulating monocytes from mice on different diets (left panel; n=9–15 mice/group) or on monocytes from ND-fed *Ldlr*^{-/-} mice after incubation with TGRL fraction from mice on WD or EVOND (right panel; n=6/group). C, Monocyte uptake of DiI-oxLDL. Total leukocytes from *Ldlr*^{-/-} mice on WD or EVOND were incubated ex vivo with DiI-oxLDL in the absence or presence of anti-mouse CD36 antibody for 1 h, and DiI signals representing monocyte uptake of oxLDL were examined by FACS (n=4/group). Data are shown as mean±SEM. *p<0.05, ***p<0.001.

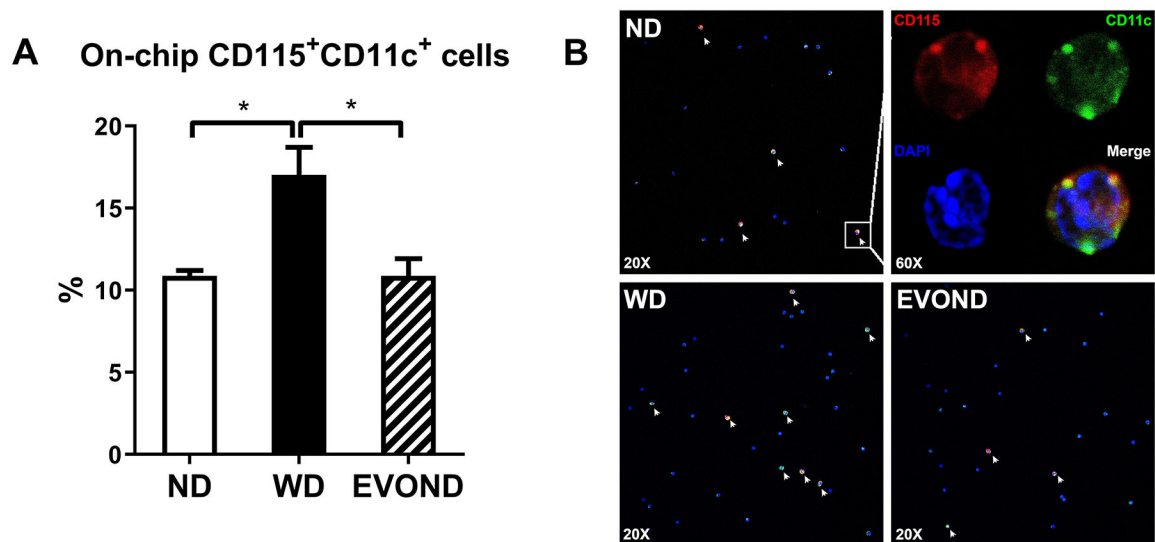


Figure 5.

Reduced on-chip adhesion of foamy monocytes from mice on EVOND vs. WD. Circulating monocytes were stained with CD115 and CD11c and perfused through VCAM-1- and E-selectin-coated chip. The number of arrested CD11c⁺ monocytes were counted and normalized by total infused monocyte number. A, Frequency of CD11c⁺ monocytes arrested on chips in the total infused monocyte. Data are shown as mean±SEM, *p<0.05, n=4/group. B, Representative images showing arrested cells on chips under flow with FITC-anti-CD11c (Green), PE-anti-CD115 (Red), and DAPI (Blue) staining. See “Ex vivo micro-flow adhesion assay” under Materials and Methods for experimental procedures. Foamy monocytes marked with white arrows were identified by CD115 and CD11c double staining.

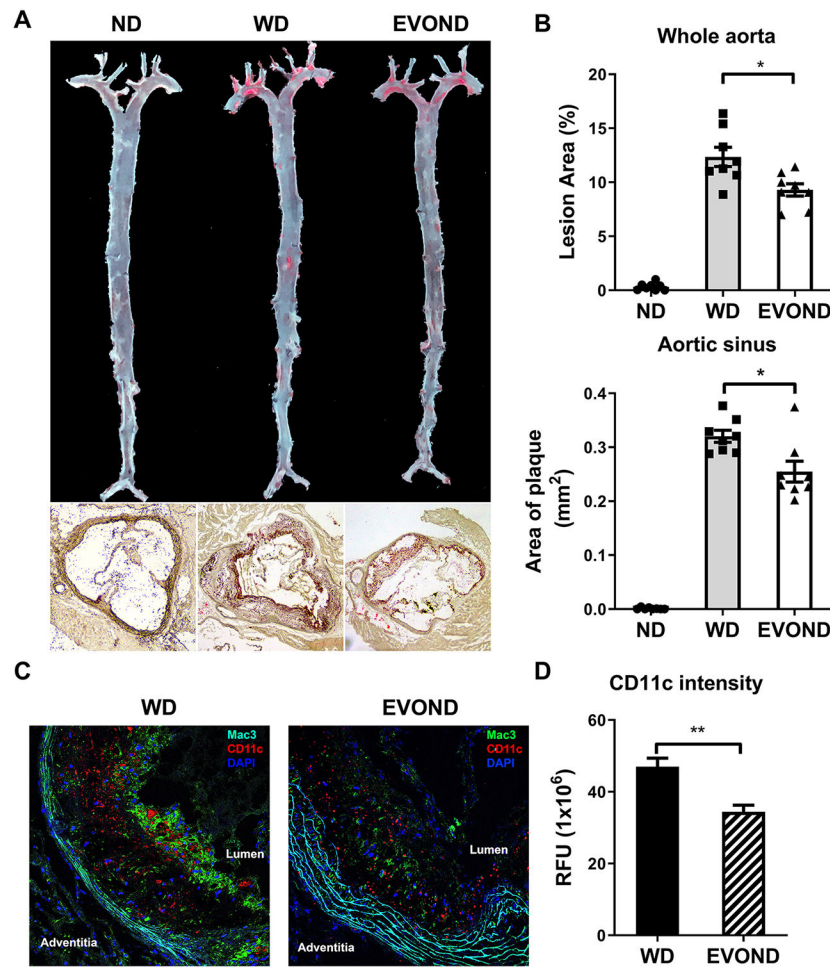


Figure 6. EVOND reduced atherosclerosis compared to WD in *Ldlr*^{-/-} mice on diets for 3 months. A, Representative en face oil red O staining of whole aorta and aortic sinus (10x original magnification). B, Statistics of plaque area of whole aorta (upper panel) and aortic sinus (lower panel) (n=8/group). C, Representative immunofluorescence staining of Mac3 (green) and CD11c (red), with DAPI staining (blue) for nuclei, in aortic sinus lesions. D, CD11c fluorescent intensity (relative fluorescent unit [RFU]) in plaque of mice from WD and EVOND groups (n=6/group). Data are shown as mean±SEM. *p<0.05, **p<0.01.